A large deformation formulation and solution with space-time finite elements

C. BOHATIER (MONTPELLIER)

THE BALANCE FORMULATION is assumed by the integration on each step of time of the evolution interval. Therefore the equilibrium is enforced on the whole step of time. The description of the deformation is an instantaneous updated Lagrangian description which is particularly suitable for large deformations. The numerical solution is made with space-time finite elements that leads to an interpolation of the unknown variables with interpolation function of time and space. The Newton–Raphson method is used and takes into account the geometry evolution. The special choice of the space-time elements allows for a frontal solution and without increasing the number of unknown variables.

1. Introduction

THE AIM OF THIS PAPER is to show that interpolation of the unknown variables by the interpolation functions of space and time leads to securing the equilibrium during the deformation process at any step of time. Therefore, it is possible to increase the increment of time (see [6]) in comparison with the classical explicit or implicit methods that split space integration and time integration (see [1, 2]).

The originality of the formulation presented here consists in using the approach that is developed in [3] and [6], but similarly to [1] and [2], it takes into account the geometry evolution at any step of the numerical solution. The unilateral contact can be tackled by numerous methods (see [4, 7, 9]). The method considered in this paper is an augmented Lagrangian method with numerical solution using Usawa's algorithm.

2. Formulation

2.1. Relative equilibrium formulation

The virtual power principle is written in the classical form

$$(2.1) \qquad \int_{\Omega} \sigma : \mathbf{D}^* d\Omega - \int_{\Omega} \rho \left(\mathbf{f} - \frac{d\mathbf{v}}{dt} \right) \cdot \mathbf{v}^* d\Omega - \int_{\partial\Omega} \mathbf{F} \cdot \mathbf{v}^* \, da = 0 \,,$$

where Ω — domain of the solid, $d\Omega$ — volume element, $\partial\Omega$ — boundary of the domain, da — surface element, ∂ — Cauchy stress tensor, D^* — virtual deformation rate tensor, $\mathbf{f}$ — external body forces, $\mathbf{v}$ — real velocity, $\mathbf{v}^*$ — virtual velocity, $-\rho \dfrac{d\mathbf{v}}{dt}$ — inertial forces, $\mathbf{F}$ — external surface forces.

We can notice that this formulation depends on the velocity field $\mathbf{v}$, on the external forces $\mathbf{F}$ and $\mathbf{f}$, on the domain Ω and its boundary $\partial\Omega(\partial\Omega \cup \Omega = \overline{\Omega})$. If the velocity field is taken as the main unknown variable, and the unknown external forces $\mathbf{F}_x$ and the domain configuration $\overline{\Omega}$ as auxiliary unknown variables, the equilibrium equation of the

problem can be written in the form

(2.2) $\phi(\mathbf{v}, \mathbf{F}_x, \overline{\Omega}) = 0$.

In various problems the unknown forces $\mathbf{F}_x$ are mainly the result of the geometrical constraints. If the mechanical linkages are considered as main, then the work of the normal component vanishes when the geometrical constraints are time-independent. However, it is possible to say that these forces $\mathbf{F}_x$ depend on the velocity field and its gradient history.

It it is required that the relation (2.2) should be satisfied for any time t during the time interval $[t_0, t_1]$ within the time of simulation $T_s(T_s \supset [t_0, t_1])$, then Eq. (2.2) results in the formulation

(2.3) $\displaystyle\int_{t_0}^{t_1} \phi(\mathbf{v}, \mathbf{F}_x, \overline{\Omega})\, dt = 0$.

Therefore, the formulation (2.3) leads to a spatial and a time integration that is divided into the three following terms:

(2.4) $I = I_1 + I_2 + I_3$,

with

$$I_1 = \int_{t_0}^{t_1} \left(\int_{\Omega} \sigma : \mathbf{D}^* \, d\Omega \right) dt = \int_{t_0}^{t_1} \int_{\Omega} \sigma : \mathbf{D}^* \, d\Omega \, dt,$$

$$I_2 = -\int_{t_0}^{t_1} \left(\int_{\Omega} \rho \left(\mathbf{f} - \frac{d\mathbf{v}}{dt} \right) \cdot \mathbf{v}^* \, d\Omega \right) dt = -\int_{t_0}^{t_1} \int_{\Omega} \rho \left(\mathbf{f} - \frac{d\mathbf{v}}{dt} \right) \cdot \mathbf{v}^* \, d\Omega \, dt,$$

$$I_3 = -\int_{t_0}^{t_1} \left(\int_{\partial \Omega} \mathbf{F} \cdot \mathbf{v}^* \, da \right) dt = -\int_{t_0}^{t_1} \int_{\partial \Omega} \mathbf{F} \cdot \mathbf{v}^* \, da \, dt.$$

The integrals I_1, I_2 and I_3 are calculated with the integration elements $d\Omega \, dt$ and $da \, dt$.

2.2. Contact conditions (Fig. 1)

$\partial\Omega_c$ — contact area between tool and work-piece, $\partial\Omega_{cc}$ — possible contact surface between tool and work-piece, P — possible contact point, P' — possible contact point, predicted by the velocity field at the beginning of the step of time, n — external normal to the tool at P'.
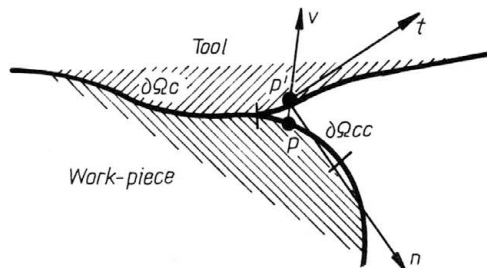

FIG. 1. Unilateral contact and its modeling.

The prediction of the possible contact point is said to be the geometrical investigation phase (see [4]). When the surfaces are discretized by facets, the predicted normal is a normal to the considered facet. When the impact point is close to several facets, it is necessary to consider all the constraints coming from these possible contact areas.

When the friction is taken into account with the unilateral contact, an augmented Lagrangian multipliers method is used for the normal components, a new integral term I_{33} with Lagrange multipliers is added to I_3, and the contribution of tangential components is included in the dissipation integral I_{32}. In mechanical terms, the contact linkages are not considered to be the main linkages.

(2.5) $$I_3 = I_{31} + I_{32} + I_{33},$$

with

$$I_{31} = - \int_{t_0}^{t_1} \int_{\partial \Omega_d} \mathbf{F_d} \cdot \mathbf{v}^* \, da \, dt,$$

$$I_{32} = - \int_{t_0}^{t_1} \int_{\partial \Omega_c} \mathbf{F_t} \cdot \mathbf{v}^* \, da \, dt,$$

$$I_{33} = - \int_{t_0}^{t_1} \int_{\partial \Omega_{cc}} \mathbf{F_n} \cdot \mathbf{v}^* \, da \, dt,$$

$\mathbf{F_d}$ — given forces, $\mathbf{F_t}$ — tangential forces on the contact area.

These friction forces lead to the dissipation processes on the contact areas. A local friction law can either depend only on the velocity field as it is formulated in the Northon–Hoff friction law (see [2]), or depend only on the normal component in the case of the Coulomb friction law (see [4]), or be a mixed formulation. The friction law can be considered as non-local (see [8]). The choice is imposed by the contact materials behaviour and their interface behaviour. $\mathbf{F_n}$ — normal contact forces, which are dependent of the solids thrust and the unilateral contact state.

If the virtual velocity field is chosen in order to allow for their work, then the normal contact forces appear as Lagrange multipliers in the expression after minimization of the Lagrangian with respect to the velocity field. When the Lagrangian of the problem is $L(\mathbf{v}, \mathbf{F})$ and $\mathbf{v}$ is a kinematically admissible velocity field and $\mathbf{F}^*$ a statically admissible normal forces field, therefore we have

(2.6) $$L(\mathbf{v}, \mathbf{F}^*) \leq L(\mathbf{v}, \mathbf{F}) \leq L(\mathbf{v}^*, \mathbf{F}),$$

$\mathbf{v}$ — minimizes $L(\mathbf{v}^*, \mathbf{F})$, $\mathbf{F}$ — maximizes $L(\mathbf{v}, \mathbf{F}^*)$.

2.3. Material behaviour

As an example, consider here the case of the viscoplastic behaviour. Then the stress tensor is a nonlinear function of the strain rate tensor. The material is assumed to be homogeneous isotropic and incompressible, and to obey the Northon–Hoff law

(2.7) $$S = 2K \frac{\mathbf{D}}{(\sqrt{3}D)^{m-1}},$$

where $\mathbf{D} = \frac{1}{2} (\mathbf{grad}\,\mathbf{v} + \mathbf{grad}^T\,\mathbf{v})$ is the Euler strain rate tensor, $D = (\frac{2}{3}\mathbf{D} : \mathbf{D})^{1/2}$ is the equivalent strain rate scalar, : is the symbol of the doubly contracted tensor product, $\mathbf{S}$ is the deviatoric part of the Cauchy stress tensor σ, m is the strain rate sensitivity, K is the material consistency.

3. Numerical solution

3.1. Space-time discretization

The classical methods consist in using a spatial discretization separated from the time discretization scheme. This fact leads us to consider various descriptions: total Lagrangian, updated Lagrangian and the instantaneous updated Lagrangian (see [1, 2]). The space time discretization leads to using in a natural way the material description with the instantaneous updated Lagrangian description. Then the Cauchy stress tensor and the Euler deformation rate tensor are defined at any time t inside the time step. The geometrical configuration is parametric and is automatically updated at each iteration (see Fig. 2). The main unknown variable, the velocity $\mathbf{v}$, is estimated by interpolation functions of space and time. The nodal values of the velocity field are defined at each node of the space-time mesh by the vector $\mathbf{V}$.
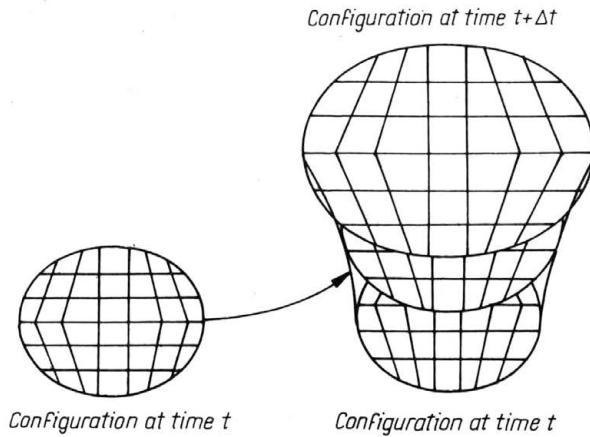

FIG. 2. Description of the domain evolution inside the step of time.

At each iteration, the new approximated domain is calculated when the new velocity field approximation is known. In the problems considered here, the contact forces appear mainly in order to take into account the unilateral contact boundary conditions. Therefore, it is not necessary to know their values accurately, and it is possible to call these unknown forces the auxiliary unknown variables.

The contact evolution could be controlled as it is made in [2], but the approach based on the Lagrangian method proposed here can better integrate the evolution contact to satisfy the equilibrium inside each step of time, for any step of time. The space-time approach of the effect of the contact term, leads to the evaluation of their variation (see [5]).

3.2. Numerical integration

The integral I_1 is obtained by computing the sum of products of the function by the weight $\overline{\omega}_i$ for all the integration points i. For instance, the numerical integral of the function Ψ over any element of the solid domain, is calculated by the expression

$$(3.1) \qquad \int_{[\Omega_n UT]} \Psi \, d\Omega \, dt = \sum \int_{[\Omega_n UT]_i} \Psi_i \, d\Omega \, dt = \sum \overline{\omega}_i \Psi_i \,,$$

where $\mathbf{V}$ is the discretized velocity vector associated to the velocity field $\mathbf{v}$, $[\Omega_n UT]_i$ is the discretized space-time sub-domain of any space-time element. At each iteration, the increment of time is fixed whereas the geometrical configuration is updated as soon as the new approximation of the velocity field is known. The spatial finite element method requires classically a reference element (see Fig. 3 and Fig. 4), then (3.1) is computed by (3.2) for any element.

$$(3.2) \qquad \int_{[\Omega_n UT]_i} \Psi_i \, d\Omega \, dt = \int_{[\Omega_n UT]_{ri}} \Psi_i J \, d\Omega_r \, dt_r \,,$$

where r is the index of the reference element, J is the Jacobian of the transformation which connects the real sub-domain to the domain of the reference element.
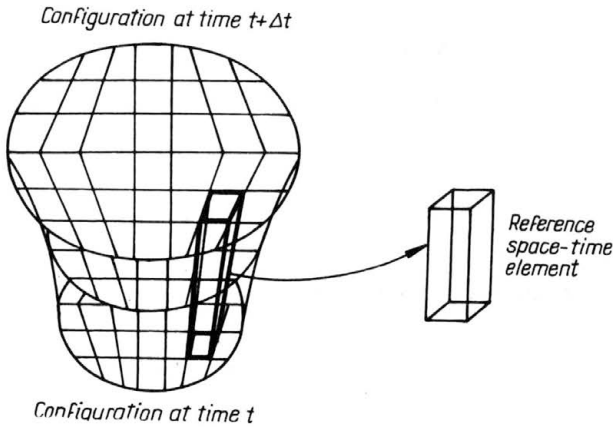

FIG. 3. Connection between the real space-time and the reference space-time element.
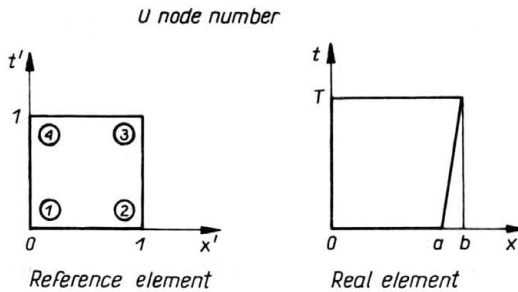

FIG. 4. Connection between reference element and real element with one dimension of space.

Therefore, the connection between the real element and the reference element leads to a numerical integration using the weight associated at the reference integration point.

3.3. An elementary example

For the sake of simplicity, let us present here an example with one dimension of space and one step of time. The connection between the real space-time element and the reference space-time element is formulated by:

The relation between t and t' is constant if a fixed increment of time is used. It is better that it can move within the deformation process in order to adapt itself to the variations of deformation gradient. At the beginning of any step of time, when the increment of time is fixed $T = t_1 - t_0$, then

$$t' = Tt .$$

The relation between the variables x and x' change at each time since the displacements and the evolution of the velocity field modify the domain. With a space-time reference element in one dimension of space, the interpolation functions associated with the domain (1×1) (see Fig. 4) are formulated:

(3.3)
$$
\begin{aligned}
N_1 &= (1 - x')(1 - t') , \\
N_2 &= x'(1 - t') , \\
N_3 &= t'x' , \\
N_4 &= t'(1 - x') .
\end{aligned}
$$

The domain evolution is estimated by the expression

(3.4)
$$x(t) = x(t_0) + \int_{t_0}^{t} \mathbf{v}\, dt ,$$

and the integral is computed according to the formula

(3.5)
$$\int_{t_0}^{t} \mathbf{v}\, dt = \Sigma \mathbf{V}_i T \int_{0}^{1} N_i(x', t')\, dt' .$$

If t' is called reduced time, the location vector is updated from the initial time of the increment by

(3.6) $$x(t) = x(t_0) + ((1 - x')V_1 + x'V_2)\left(t' - \frac{t'^2}{2}\right)T + (x'V_3 + (1 - x')V_4)\frac{t'^2}{2}T .$$

It is interesting to notice that
if $t' = 1$ and $x' = 1$, then

$$x(t) = x(t_0) + (V_2 + V_3)\frac{T}{2} .$$

This result is similar to that in [1, 2].

The Jacobian of the transformation is evaluated by the formula

(3.7) $$J = \left| \frac{D(x, t)}{D(x', t')} \right| = T\left(a + T\left((V_2 - V_1)\left(t' - \frac{t'^2}{2}\right) + (V_3 - V_4)\frac{t'^2}{2}\right)\right) .$$

REMARKS

J does not depend on x' because of the linear relation with x (element of C_0). When one integration point is chosen in $x' = \frac{1}{2}$ and $t' = \frac{1}{2}$, its expression becomes

$$J = T\left(a + T\left(\frac{3}{8}(V_2 - V_1) + \frac{1}{8}(V_3 - V_4)\right)\right).$$

At $t' = 0$, $J = aT$; at $t' = 1$, $J = T(a + \frac{T}{2}((V_2 - V_1) + (V_3 - V_4)))$.
Moreover the boundary conditions are $V_1 = V_4 = 0$, then

$$J = T\left(a + \frac{T}{2}(V_2 + V_3)\right).$$

The mesh evolution is the same as that considered in [1, 2]. Therefore, when a space-time element belonging to C_0 is chosen with only two values of time and one integration point, the integration can be compared with the one developed in [1, 2] but with a spatial integration over an intermediate configuration.

3.4. Unilateral contact

The problem of the unilateral contact is solved using the Usawa's algorithm with the mixed formulation that comes from the Lagrange method (2.6). v minimizes $L(\mathbf{v}^*, \mathbf{F})$ solution by a fixed point method or the Newton–Raphson method; $\mathbf{F}$ maximizes $L(\mathbf{v}, \mathbf{F}^*)$ solution by a projected gradient method.

At each step of time and for each iteration, the velocity field is estimated after having fixed an approximation of the contact forces. Therefore the problem becomes a velocity problem that is similar to that solved in [2]. The approximations of the velocity field and the contact forces are alternately calculated during the iteration process. The control is made by the convergence of the velocity field. At the first iteration the contact force at any possible contact point is estimated at zero. At the iteration k, it is evaluated by

$$(3.8) \qquad F_n^{(k+1)} = \text{Proj } F_{n \geq 0}(F_n^{(k)} - \mu \int_{t_0}^{t_1} F_n^* \cdot v_n \, dt$$

with F_n^* — virtual admissible normal force.

For all the possible contact points between the body and a rigid obstacle, F_n^* is formulated by

$$(3.9) \qquad F_n^* = \frac{1}{2}(-1 + \text{sgn}(h + u_n)),$$

v_n, u_n, F_n are the components along the external normal to tool (opposite to the work-piece), h is the initial gap between the tool and the work-piece at the beginning of the considered step of time, on the normal to the tangential plane at the impact point estimated at the first iteration.

In order to improve the convergence of Usawa's algorithm, the Lagrangian is augmented by a penalisation term that comes from the unilateral contact constraint. Then, an extra term I_{34} appears in the integral I_3

$$(3.10) \qquad I_{34} = \frac{1}{2\varepsilon} \int_{t_0}^{t_1} \int_{\partial \Omega_c} \left(\frac{h}{T} - v_n\right) j(h - u_n) \cdot v^* \, da \, dt,$$

where

$$j(u_n) = 0 \quad \text{si} \quad h - u_n \geq 0, \quad j(u_n) = 1 \quad \text{si} \quad h - u_n < 0.$$

3.5. Assembling (Fig. 5)

FIG. 5. Influence area for the node with coordinates x_3, t_3.

3.6. Solution methods

FIRST METHOD

When a space-time element with only two nodal values of time is chosen, the band is "hyper-wide" (see [3]). The frame of the assembling can be drawn in the following form:

$$
\begin{bmatrix}
A(V_1,V_2) & B(V_1,V_2) & & & & \\
C(V_1,V_2) & D(V_1,V_2)+A(V_2,V_3) & B(V_2,V_3) & & & \\
& C(V_2,V_3) & D(V_2,V_3) & & & \\
\hline
& & & B(V_{m-1},V_m) & & \\
& & & D(V_{m-1},V_m)+A(V_m,V_{m+1}) & B(V_m,V_{m+1}) & \\
& & & C(V_m,V_{m+1}) & D(V_m,V_{m+1}) &
\end{bmatrix}
\times
$$

$$
\times
\begin{bmatrix}
V_1 \\ V_2 \\ V_3 \\ \cdots \\ V_{m-1} \\ V_m \\ V_{m+1} \\ \cdots
\end{bmatrix}
=
\begin{bmatrix}
F_1 \\ F_2 \\ F_3 \\ \cdots \\ F_m \\ F_{m-1} \\ F_{m+1} \\ \cdots
\end{bmatrix}
$$

V_m is the discretized velocity vector at time t_m. It contains all the components of velocity at the nodes.

SOLUTION ALGORITHM

The velocity field solution consists here in solving the successive nonlinear problems that contain the same number of unknown variables as the problems solved in [1, 2]. When the behaviour is viscoplastic, then the algorithm can be used in the following manner:

Problem for step 1 of time

$$B(V_1,V_2)V_2 = F_1(V_1,V_2) - A(V_1)V_1.$$

Problem for step 2 of time

$$\mathbf{B}(\mathbf{V}_2, \mathbf{V}_3)\mathbf{V}_3 = \mathbf{F}_2(\mathbf{V}_1, \mathbf{V}_2, \mathbf{V}_3) - (\mathbf{D}(\mathbf{V}_1, \mathbf{V}_2) + \mathbf{A}(\mathbf{V}_2, \mathbf{V}_3))\mathbf{V}_2 - \mathbf{C}(\mathbf{V}_1, \mathbf{V}_2)\mathbf{V}_1$$

. . . .

Problem for step m of time

$$(3.11) \quad \mathbf{B}(\mathbf{V}_m, \mathbf{V}_{m+1})\mathbf{V}_{m+1} = \mathbf{F}_m(\mathbf{V}_{m-1}, \mathbf{V}_m, \mathbf{V}_{m+1}) - (\mathbf{D}(\mathbf{V}_{m-1}, \mathbf{V}_m)$$
$$+ \mathbf{A}(\mathbf{V}_m, \mathbf{V}_{m+1}))\mathbf{V}_m - \mathbf{C}(\mathbf{V}_{m-1}, \mathbf{V}_m)\mathbf{V}_{m-1}.$$

If at time t_2 an approximation of $\mathbf{V}_2$, for instance $\mathbf{V}_1$ is considered in order to estimate $\mathbf{B}(\mathbf{V}_1, \mathbf{V}_2)$ and $\mathbf{F}_1(\mathbf{V}_1, \mathbf{V}_2)$, then the Problem 1 is a linear problem with the unknown variable $\mathbf{V}_2$. The new approximation is then used in $\mathbf{B}$ and $\mathbf{F}$ and so on, until the convergence criteria are satisfied.

It is important to notice that in the general case $\mathbf{F}_m$ depends on $\mathbf{V}_{m-1}$, $\mathbf{V}_m$, $\mathbf{V}_{m+1}$ because of the updating of the geometrical configuration and the expression of the dissipation. Such a solution called the fixed point method could have some difficulties with converging, particularly when the increment of time is large.

SECOND METHOD

The discretization leads to an iterative solution of Eqs. (3.12) and (3.13). The computation of the successive approximations of the velocity leads to the evaluation of the unknown geometrical configuration.

When it is found that the problem can be solved by a frontal method, the solution of Eqs. (3.12), (3.13) is done by the Newton–Raphson method. On the first step of time the initial configuration is known, and $\mathbf{V}_2$ is the main unknown variable. For the next step of time the first approximation comes from the previous calculation.

$$(3.12) \qquad\qquad\qquad \mathbf{H}(\mathbf{V}_n)\delta\mathbf{V}_n = -\lambda\mathbf{g}(\mathbf{V}_n),$$
$$(3.13) \qquad\qquad\qquad \mathbf{V}_{n+1} = \mathbf{V}_n + \delta\mathbf{V}_n.$$

Assume that $\mathbf{V}_n$ is the discretized velocity at iteration n, then the gradient $\mathbf{g}(\mathbf{V}_n)$ and the $\mathbf{H}(\mathbf{V}_n)$ are formulated by the expressions

$$(3.14) \quad \mathbf{g}(\mathbf{V}_n) = \int\limits_{[\Omega_n UT]} \left(\left(\sigma : \frac{\partial\mathbf{D}}{\partial\mathbf{V}} - \rho\left(\mathbf{f} - \frac{dv}{dt}\right)\right) \frac{\partial\mathbf{v}}{\partial\mathbf{V}}\right) d\Omega\, dt - \int\limits_{[\partial\Omega_n UT]} \mathbf{F} : \frac{\partial\mathbf{v}}{\partial\mathbf{V}}\, da\, dt,$$

$$(3.15) \quad \mathbf{H}(\mathbf{V}_n) = \int\limits_{[\Omega_n UT]} \left(\frac{\partial\sigma\partial\mathbf{D}}{\partial\mathbf{D}\partial\mathbf{V}} : \frac{\partial\mathbf{D}}{\partial\mathbf{V}} + \frac{\partial\rho\left(\mathbf{f} - \dfrac{dv}{dt}\right)}{\partial\mathbf{V}} \frac{\partial\mathbf{v}}{\partial\mathbf{V}} + \sigma : \frac{\partial\mathbf{D}}{\partial\mathbf{V}}\,\mathrm{div}\left(\frac{\partial\mathbf{v}}{\partial\mathbf{V}}\right)\right) d\Omega\, dt$$

$$- \int\limits_{[\partial\Omega_n UT]} \left(\frac{\partial\mathbf{F}\partial\mathbf{v}}{\partial\mathbf{v}\partial\mathbf{V}} : \frac{\partial\mathbf{v}}{\partial\mathbf{V}} + (\mathbf{T} + \mathbf{F})\frac{\partial\mathbf{v}}{\partial\mathbf{V}}\,\mathrm{div}_a\left(\frac{\partial\mathbf{v}}{\partial\mathbf{V}}\right)\right) da\, dt,$$

where div_a is the divergence of $\partial\Omega$, $[\Omega_n UT]$ and $[\partial\Omega_n UT]$ represent, respectively, the body space-time domain and its boundary $0 < \lambda \leq 1$ is chosen in order to have

$$\|\delta\mathbf{V}_{n+1}\| < \|\delta\mathbf{V}_n\| \quad \text{(see [1] and [2])}$$

REMARKS

The Hessian is symmetrical:

if $\mathbf{T}$ is independent of $\mathbf{v}$, then the Hessian is independent of the boundary term;

if the material is incompressible, then div $\left(\dfrac{\partial \mathbf{v}}{\partial \mathbf{V}}\right) = 0$. During the iteration process, the material behaviour evolution is controlled and the internal variables, function of the history of gradient of velocity (for instance stress hardening), are updated.

The relations between the solution of Eq. (3.11) at step of time m and the one of Eqs. (3.12), (3.13) are given by

(3.16) $$\mathbf{g} = \mathbf{B}\mathbf{V}_{m+1} + (\mathbf{D} + \mathbf{A})\mathbf{V}_m + \mathbf{C}\mathbf{V}_{m-1}\,,$$

(3.17) $$\mathbf{H} = \mathbf{B} + \frac{\partial}{\partial \mathbf{V}_{m+1}}(\mathbf{A} + \mathbf{B} - \mathbf{F})\,.$$

In short, the algorithm of solution proposed here can be written as follows.

Repeat for any step of time

$k = 1,\ \mathbf{V}^1_{m+1} = \mathbf{V}_m,$

repeat,

estimated $\mathbf{F}^{(k)}_n$,

solve the equation for unknown variable $\mathbf{V}^k_{m+1}$,

calculate $E = \dfrac{\|\mathbf{V}^{k+1}_{m+1} - \mathbf{V}^k_{m+1}\|}{\|\mathbf{V}^1_{m+1}\|},$

$k = k + 1,$

until ($E \le \varepsilon_{\mathbf{v}}$ and $g(\mathbf{v}) \le \varepsilon_g$).

Until the limit of the deformation process.

4. Conclusion

The use of the space-time finite element enables the spatial and time interpolation that can describe the relative equilibrium for any time instant inside each time step.

This approach is particularly interesting for the study of large deformation and for the metal forming applications. It leads to improving the velocity formulation, based on an instantaneous updated Lagrangian description presented in [1, 2].

The application of the space-time finite element should make it possible to consider any problems involving fast motion of the objects, and their internal or boundary behaviour. The evolution of mesh can be taken into account inside a step of time when the evolution of the deformation process could lead to inaccuracy. This approach with space-time finite element allows to increase the increment of time without increasing the number of unknown variables. Therefore, at the same accuracy, the computation time decreases in comparison to the classical methods.

References

1. C. BOHATIER and J. L. CHENOT, *F. E. M. for non-steady-state large viscoplastic deformation*, Int. J. for Num. Meth. in Enging. 1985.
2. C. BOHATIER and J. L. CHENOT, *F. E. M. for non-steady-state large viscoplastic deformation with sliding or evolving contact boundary conditions*, Int. J. for Num. Meth. in Enging. 1989.
3. C. I. BAJER and C. G. BONTHOUX, *State-of-art in true space-time finite element method*, The Shock and Vibration Digest, Vibr. Institute, 20, 4, April 1988.
4. M. JEAN and G. TOUZOT, *Implementation of unilateral contact and dry friction in computer codes dealing with large deformations problems*, J. M. T. A. Sup. No. 1, 7, pp. 145–160, 1988.

5. J. J. MOREAU and P. D. PANAGIOTOPOULOS, *Nonsmooth mechanics and applications*, pp. 1–82, Springer Verlag, Wien–New York 1988.

6. C. BAJER, R. BOGACZ and C. BONTHOUX, *Adaptative space-time elements in the dynamic elastic-viscoplastic problem*, Comp. and Structures (to be published).

7. J. H. HEEGAARD and A. CURNIER, *An augmented Lagrangian method for large slip contact problems*, Euromech 273, La Grande Motte, France 1990.

8. G. DUVAUT, *Loi de frottement non locale* [Nonlocal friction law], J. M. T. A. Special Edition, p. 73–78, 1982.

9. *Euromech 273, Unilateral contact and dry friction*, Proceedings La Grande Motte, France, June 1st 1990.

LMGMC MONTPELLIER — USTL, MONTPELLIER, FRANCE.